Arabian Journal of Chemistry (2020) **13**, 6493–6509

King Saud University

Arabian Journal of Chemistry

www.ksu.edu.sa
www.sciencedirect.com

ORIGINAL ARTICLE

An innovative impurity profiling of Avanafil using LC and LC-MS/MS with in-silico toxicity prediction

Mital Patel [a,c], **Charmy Kothari** [a,*], **Vivek Vyas** [b]

[a] *Department of Pharmaceutical Analysis, Institute of Pharmacy, Nirma University, Ahmedabad, India*
[b] *Department of Pharmaceutical Chemistry, Institute of Pharmacy, Nirma University, Ahmedabad, India*
[c] *Shobhaben Pratapbhai Patel School of Pharmacy and Technology Management, SVKM's NMIMS-Deemed to be University, Mumbai 400056, India*

Received 5 April 2020; accepted 3 June 2020
Available online 18 June 2020

KEYWORDS

Avanafil;
LC-MS/MS;
Impurity profile;
Fragmentation;
Stability indicating method

Abstract Degradation of the drug can lead to the formation of toxic substance hence drug quality and stability is a major concern by pharma regulators. A Selected phosphodiesterase type 5 inhibitor drug Avanafil (AV) structure has amide, arylchloro and hydroxide as functional groups which can easily eliminated during hydrolysis. Henceforth, thoroughly chemical stability of AV was carried out according to ICH guideline Q1A (R2). The drug and marketed tablet formulation undergoes degradation in hydrolytic (acid, base, neutral), thermal, photolytic, oxidative conditions and forms a total new sixteen degradation products (D.P.s) which were identified by LC, characterized by LC-MS/MS and probable degradation mechanism for each stress conditions are proposed. All sixteen D.P.s were identified by optimized LC conditions; C18 column using 10 mM ammonium acetate: ACN (60:40, v/v), pH 4.5 as mobile phase at 0.9 mL min^{-1} of flow rate, 239 nm wavelength at 20 °C column temperature and the method being LC-MS compatible characterized by LC-MS/MS confirmed by relative retention time (RRT). The structure of D.P.s was confirmed from the fragmentation pattern obtained by LC-MS/MS and further probable degradation mechanism for each stress condition is proposed. The drug and its marketed tablet formulation showed similar degradation peaks which were confirmed using RRT, photodiode array (PDA) and LC-MS. Drug degradation happens due to nucleophilic substitution reaction, amide hydrolysis, electron withdrawing properties of amide, dechlorination and bond cleavage due to energy. The amide group in AV structure can undergo hydrolysis, while due to aryl chloride and hydroxide group in structure

* Corresponding author at: Department of Pharmaceutical Analysis, Institute of Pharmacy, Nirma University, Sarkhej-Gandhinagar Highway, Post: Chandlodia, Via –Gota, Ahmadabad 382 481, Gujarat, India.
E-mail address: charmy.kothari@nirmauni.ac.in (K. Charmy).
Peer review under responsibility of King Saud University.

Production and hosting by Elsevier

https://doi.org/10.1016/j.arabjc.2020.06.007

it undergoes photodecomposition. A comprehensive stress study reveals that AV is more prone to degrade in light, temperature and moisture; hence AV requires proper storage condition temperature below 25 °C with protection to light and moisture. In silico toxicity prediction of physicochemical properties revealed that all the physicochemical parameters of impurities were within the acceptable limit which indicates that no impurity is at any risk of toxicity. In detail, the LC-MS/MS compatible AV degradation study is fully validated as per ICH Q2 (R1) guideline.

1. Introduction

Building blocks of the pharmaceutical industry are quality, safety and efficacy. Stability of active pharmaceutical ingredient (API) and formulation is a prime requirement for any industry to study half-life, shelf life and expiry period of the drug. As per ICH Q1A (R2) (ICH, 2005a) stress degradation is the process to find out the stability of drug molecule in presence of variable chemical and environmental conditions. Further identification and characterization of degradation products (D.P.s) will help to find out inherent stability study of a drug, half-life, shelf life and expiry period of the drug (Bakshi and Singh, 2002). All the drug substances and drug products tend to degrade in different environmental conditions (light, temperature, moisture, heat, etc.) as discussed by the Bakshi in a harmonized way. In detail drug stress testing by LC-MS/MS provides information about structures of D.P.s, and plausible degradation mechanisms which aids to know the toxicity and side effects. In literature, there are many reports on forced degradation study and structural elucidation of drugs by analytical methods including hyphenated techniques. (Jain and Basniwal, 2013; Kalariya et al., 2015b; Kurmi et al., 2016; Narayanam et al., 2013; Ramesh et al., 2014; Shankar et al., 2019; Singh et al., 2012). From degradation study data plausible degradation mechanism can establish. The degradation can be due to hydrolysis, oxidation, rearrangement, substitution, dimerization, and removal of halo atoms. (Bandichhor, 2014; Li et al., 2014; Modhave et al., 2011; Narayanam and Singh, 2014; Rao et al., 2014; Srinivasu et al., 2010). The drug substance degradation profile is handy for clinical study, preclinical study, drug product manufacturing, and marketing. (Kalariya et al., 2015a; Shankar et al., 2019).

Phosphodiesterase type 5 (PDE 5) inhibitors are used in the treatment of erectile dysfunction (ED) and explored for the treatment of pulmonary hypertension (Ferguson and Carson, 2013). Avanafil (AV) as PDE 5 inhibitor drug, developed by Mitsubishi Tanabe Pharma Corporation (Osaka, Japan) to treat erectile dysfunction. Chemically it is [(s) - (4-[(3chloro-4-methoxybenzyl) amino]-2-[2-(hydroxymethyl)-1pyrrolidinyl] - N - (2 pyrimidinyl methyl) − 5-pyrimidine carboxamide)] (Kotera et al., 2012; Zurawin et al., 2016). AV is soluble in acetonitrile (ACN), methanol, and dimethyl sulfoxide (DMSO) but insoluble in water. AV has two pKa values, which are 11.84 (acidic) and 5.5 (basic).

The detail AV literature review reveals that few reports were published related to pharmacological action as PDE 5 inhibitor (Ferguson and Carson, 2013), tolerability and pharmacokinetic study of AV with LC-MS/MS method (Jung et al., 2010). Several analytical methods have been reported for the AV determination by UV spectroscopy method (Savaliya et al., 2013), simultaneous estimation of Avanafil and Dapoxetine with the HPLC method (Mangukiya et al., 2014) and multivariate analysis of Avanafil and Dapoxetine (Patel and Kothari, 2016). A Few reports on HPLC stability methods have been reported for the determination of AV (Bhumik et al., 2015; Kumar et al., 2017; Can, 2018). Bhumik et. al have developed a stability LC method for AV which can merely identify AV peak, hence it does not fulfill the purpose of the stability-indicating analytical method (SIAM). Report by Kumar et al. focused on an AV stability study in certain degradation conditions via gradient method. The reported method reveals the separation of AV but not effective for the separation of all degradation peaks. Recently published report by Can focused on the identification of two related substances and one degradation product of AV by LC-MS-IT-TOF (Can, 2018). However, the reported method was not efficient to separate degradation products due to a lack of method sensitivity. The reported method identified two related substances and one degradation product using LC-MS/MS and had predicted structures.

To best of our knowledge to date, not a single report available for a comprehensive impurity profile with full validation exists for AV, which is crucial for quality control of drugs, to establish critical steps during synthesis and to maintain quality of AV during the pharmaceutical process. Hence, the key aim of this study is to develop a method for better identification and characterization of D.P.s of AV, elseways AV monograph is not available in any pharmacopeias. The major rewards of the developed method over reported one were of use of a single method to separate and identify new sixteen D.P.s, method LC-MS/MS compatible, method sensitivity and applicability for marketed formulation. A novel, isocratic, analytical, LC-MS/MS compatible method was developed to separate all possible AV degradation products in different conditions; subjected aimed at LC-MS/MS characterization and plausible fragmentation.

2. Experimental

2.1. Chemical and reagent

Analytically pure (99.9%) reference standard of Avanafil (AV) was received as a gratis sample from Sunrise Remedies Pvt., Ltd. (Ahmedabad, India) and Om laboratory (Ahmedabad) along with a certificate of analysis. The marketed tablet formulation of Avanafil (Avana) was procured as a gratis sample from Sunrise Remedies Pvt., Ltd. (Ahmedabad, India). HPLC grade acetonitrile (ACN) and glacial acetic acid were procured from Merck, Mumbai, India. Ammonium acetate of HPLC

grade was purchased from Finar Chemicals Pvt. Ltd. (Ahmedabad, India). HPLC grade water (triple distilled water) was prepared in the laboratory by distillation assembly. Hydrochloride acid, sodium hydroxide and hydrogen peroxide (30% w/v) used for stress degradation studies were of analytical grade procured from CDH chemicals, Delhi, India.

2.2. Apparatus and instrumentation

pH meter (Accurate scientific, Ahmedabad) was used to check the pH of all solutions. Other equipment used for studies were melting point apparatus (T060160, EIE Instruments Pvt. Ltd., Ahmedabad, India), precision analytical balance (CX 220, citizen, USA), sonicator (D-compact, EIE Instrument Pvt. Ltd., Ahmedabad, India) and variable micropipette (Axiva Sichem Biotech, Delhi). Precision water bath equipped with MV controller (EIE 406, EIE, Instrument Pvt. Ltd, Ahmedabad, India) was used for degradation studies in the solution state. Fourier transform infrared spectrometer (FTIR) (JASCO FT/IR − 6100 series, Jasco, Japan) was used for the identification of functional groups. The membrane filters 0.22 μm (Axiva sichem biotech, Delhi), and syringe filters 0.45 μm were used for filtration.

The Agilent 1260 Infinity HPLC (Agilent Technologies, USA) equipped with an autosampler, a quaternary pump, a UV detector, and a column compartment were used during the study. Jasco HPLC (Jasco analytical instruments, USA) equipped with PDA (Photodiode array) detector was used for peak purity calculation. LC column Nucleosil C18 (250 × 4.6 mm, 5 μm) was used for better separation. LC-MS/MS studies were carried out using MS (LTQ XL™ Linear ion trap mass spectrometer), in which the LC part consisted of autosampler HPLC and MS system consisted of LCQ Fleet Ion Trap LC/MS^n (Thermo Scientific, USA). The Xcalibur software used for the data processing. For MS^n experiments, the LTQ-XL-MS instrument (Thermo Scientific, USA) was used. The mass spectra were acquired and processed using Xcalibur software. The mass parameters used were mass range, 50–2000 amu; ion source (IS), 4500 v; declustering potential (DP), 20 V; entrance potential (EP), 10 V; nebulizer gas as air at a pressure of 25 psi and curtain gas as nitrogen at a pressure of 35 psi.

2.3. Chromatographic conditions

The AV stability indicating method was developed based on preliminary trials and drug physicochemical properties. Initially, ACN with water in different ratios was tried. The better separation achieved by the addition of buffer and the buffer pH should be selected in the range of ±2 of pKa of the drug. AV has pKa value 5.54 hence, the buffer pH was set between ±2 of pKa; as in that range nearly 100% of the drug is ionized or unionized which is suitable for better seperation. A further change in the organic phase ratio affects degradation peaks retention time and column temperature change can affect on elution time due to change in viscosity of the mobile phase with temerature. After several trials isocratic, novel and specific method was optimized; this fulfills all criteria according to ICH guideline. The chromatographic conditions were optimized using Hypersil, C18 (250 × 4.6 mm, 5 μm) column with a mobile phase composed of 10 mM ammonium acetate buffer (A) (pH 4.5, adjusted with acetic acid): ACN (B) (A: B, 60:40, v/v) at flow rate of 0.9 mL min^{-1}. The column temperature, injection volume, and detector wavelength were at 20 °C, 10 μL and 239 nm, respectively. The optimized and fully validated chromatographic conditions were MS compatible hence further subjected to LC-MS studies.

2.4. Mass spectrometric conditions

LC-MS: The mass spectrometer conditions were optimized by a preliminary direct infusion of standard drug solution (10 μg mL^{-1}) into the ESI-MS system at a flow rate of 10 μL hr^{-1}, and all ion optics were optimized. General MS adjustments were set as follows: drying gas flow, 12 L min^{-1}; capillary voltage, 3500 V; desolvation temperature, 350 °C; nebulizer, 36 psi; ion change control (ICC) smart target, 150000; collision gas Ar at 20 Da collision energy (CE) [if requires increments of 5% until the intensity of the precursor ion is less than 5% of the intensity of the product ions] and max accumulation time, 150 ms used throughout the analysis. Initially, the precursor ion (m + 1) values were obtained using LC-MS studies with respect to the retention time of parent drug and it's all D.P.s. Subsequently, the MS/MS study was performed for each D.P.s to determine product ion and its fragmentation pattern.

2.4.1. MS/Ms

LC-MS and MS^n studies were performed in an ESI positive mode (ES+). Various MS/TOF parameters were sequentially altered to obtain the molecular ion peak of the drug and its fragment. AV was subjected to the MS system at a concentration of 10 μg mL^{-1} prepared in acetonitrile in positive electrospray ionization (ESI) mode in the mass range of 50–900 Da. High purity nitrogen was used as a nebulizer and auxiliary gas. The fragmentation profile of the drug was established by caring out mass spectral studies on AV, while multi-stage (MS^n) mass studies were carried out up to MS^5 to determine the origin of each fragment.

2.5. Stress studies for generation of degradation products

Stress degradation was carried out in different conditions like as hydrolysis (acidic, basic and neutral), oxidative, photolytic, and thermal according to the recommendations in ICH Q1A (R2). The stress studies were carried out by preparing the AV solution of 1 mg mL^{-1} in the respective stressor. Acetonitrile (2 mL) was added to dissolve 10 mg drug and then the volume was made up to 10 mL with respective stressors. From that, 0.1 mL of sample was withdrawn at suitable time intervals and neutralized with acid/alkali and/or diluted up to 1 mL with ACN: H_2O (50:50, v/v) to get the concentration (100 μg mL^{-1}) then injected in HPLC.

Different degradation conditions as the molar concentration of stressor, temperature, and stress duration were selected based on initial trial results, which reveals the formation of primary D.P.s. Different degradation conditions Hydrolytic (acidic and alkaline) degradation study was carried out by refluxing the drug in 1 N concentrations of HCl and NaOH at different temperatures as 60, 70, and 80 °C, while neutral hydrolysis was performed in an equal mixture of water and ACN. For oxidative degradation study, the drug was subjected

to 1%, 6%, and 10% peroxide at room temperature. Thermal stress degradation was carried out by exposing the solid drug as a thin layer in the petri-dish for 7 hr and as in solution form, an equal mixture of water and ACN was used and kept for 5 hr in an oven at 60 °C. Photolytic degradation study was carried out in the solid drug for 8 hr as well as drug solutions (an equal mixture of water and ACN) for 6 hr in direct sunlight. For Photodegradation comparison, a solid sample was placed in a photostability chamber at 1.2 million Lux hr for 6 hr. All stressed samples were kept in the amber color vial at the refrigerator until analysis.

The marketed formulation was also subjected to all degradation conditions. All stressed samples were collected, neutralized, and filtered through a 0.22 μm pore size membrane syringe filter before LC and LC-MS/MS analysis.

2.6. In silico studies

In silico study was carried out for the impurities for the prediction of physicochemical parameters like cLogP, Solubility (LogS), topological polar surface area (TPSA). Prediction of toxicity risk (*in silico*) was also carried out for the toxicity factors like mutagenicity, tumorigenicity, irritant, and reproductive effects using OSIRIS property explorer which uses Chou and Jurs algorithm, based on computed atom contributions. This software allows to underline properties with high risks of undesired effects such as mutagenicity, poor intestinal absorption, or drug conform behavior via different customization features. The OSIRIS property explorer calculates on-the-fly various drug-relevant properties whenever a structure is valid. Prediction results are valued and color-coded. Properties with high risks of undesired effects like mutagenicity or poor intestinal absorption are shown in red. Whereas a green color indicates drug-conform behavior. A working Java Runtime Environment (JRE) must be installed on the computer.

3. Result and discussion

3.1. LC separation of the drug and degradation products

The SIAM was developed and an optimized chromatographic condition (as described in Section 2.3) was used for hydrolysis, oxidative, photolysis, and thermal degradation conditions. A total sixteen D.P.s were found during different degradation conditions as shown in overlay chromatogram Fig. 1. The degradation results reveals that % degradation of AV found 21.71–25.62% in acidic condition; 20.00–25.00% in alkaline condition; 14.00–19.21% in neutral condition; 16.25–30.52% in oxidative hydrolysis; 22.39–28.96% in photolytic and 28.00–28.50% in thermal degradation. The drug (AV) found sensitive towards thermal, photolytic, oxidative, and hydrolytic conditions according to the AV stress degradation study (Table 1). The degradation was confirmed from the additional peaks achieved in the respective chromatogram and also by the reduction in the area of AV in each condition when compared with their area at zero time. The mass balance was calculated from the AV and all the D.P.s responses obtained after stress studies. Mass balance found greater than 90 for alkaline, photolytic, and thermal degradation conditions. While for acid and oxidative degradation it was 89 and 82 respectively, due to loss of some mass during degradation as seen in Table 1.

Amongst all the degradation conditions, the order of degradation behavior (based on average % degradation in each condition) observed was

Thermal > Photolytic > Oxidative > Hydrolytic (acid, alkaline and neutral)

The optimized LC method was compatible with LC-MS, hence subjected to LC-MS/MS study for AV degradation products. In different degradation conditions (acidic, alkaline, oxidative, photolytic, and thermal), various D.P.s were found. Nomenclature of formed D.P.s in different condition were given based on their Rt (retention time). Found D.P.s in LC chromatogram for the acid condition D.P. I, III, IV, VIII, XI, XIII and XIV; in alkaline condition D.P. I, III, IV, VIII, XI, XIII, XIV and XV; in neutral degradation of the drug formation of D.P.s I, III, IV, VIII, XIII and XIV; in oxidative degradation of the drug formation of D.P.s VI, XII, XIII, and XIV; in photolytic degradation D.P. II, V, VII, X, XIII, XIV and XVI and in thermal degradation D.P. II, V, IX, XIII, and XIV as shown in Fig. 1, Table 2. For additional confirmation of LC degradation peaks by LC-MS/MS peaks, RRT (relative retention time) and PDA (Photodiode array) data were used.

The degradation pattern of AV in photolytic and thermal conditions was found similar in liquid state and solid-state. Common D.P.s for acid and alkaline hydrolysis are I, III, IV, VIII, XI, XIII and XIV. Common D.P.s between acid, alkaline and neutral degradation are I, III, IV, VIII, XIII and XIV. At last for photolytic and thermal degradation found common D.P.s are II, V, XIII and XIV. Besides, AV XIII and AV XIV were common D.P.s in all conditions. The AV sixteen D.P.s were identified and characterized by LC-MS/MS and fragmentation pattern. The D.P.s structure were proposed based on MS/MS data and MS^n fragmentation.

3.2. Mass fragmentation behavior of AV

AV Fragmentation by MS/MS studies showed up to MS^5. AV was analyzed in positive ion mode by direct flow injection using ACN: water (1:1, v/v) mixture as the solvent through MS^n spectra to determine the origin of each fragment. Line spectra of drugs, obtained in MS and MS^n studies are shown in **Supplementary Fig S1**. The best possible molecular formula and exact masses for the fragments were calculated using an elemental composition calculator. The same are listed in Table 2.

The MS/MS spectrum of AV is as shown in **Supplementary Fig S1**. AV having a molecular formula of $C_{23}H_{26}ClN_7O_3$ (m/z 483.95). The fragment of AV (m/z 483) with m/z 484.22 was formed as an M + 1 peak, the fragment m/z 485.97 formed due to M + 2 peak and the fragment with m/z 506.14 was formed as a sodium adduct since its mass was approximately 1 Da (Da), 2 Da (Da) and 23 Da (Da) higher than the molecular ion peak. The mass peak of AV shows chloro pattern (1:3) in spectra which confirms the presence of chlorine in structure. MS/MS spectra shows that AV m/z 484.22 further fragment in to m/z 375.09, m/z 357.10, m/z 342, m/z 329.14 and m/z 155.12. From the MS/MS spectra, a postulated fragmentation pattern was derived as shown in Fig. 2. From drug AV, MS^2 fragment

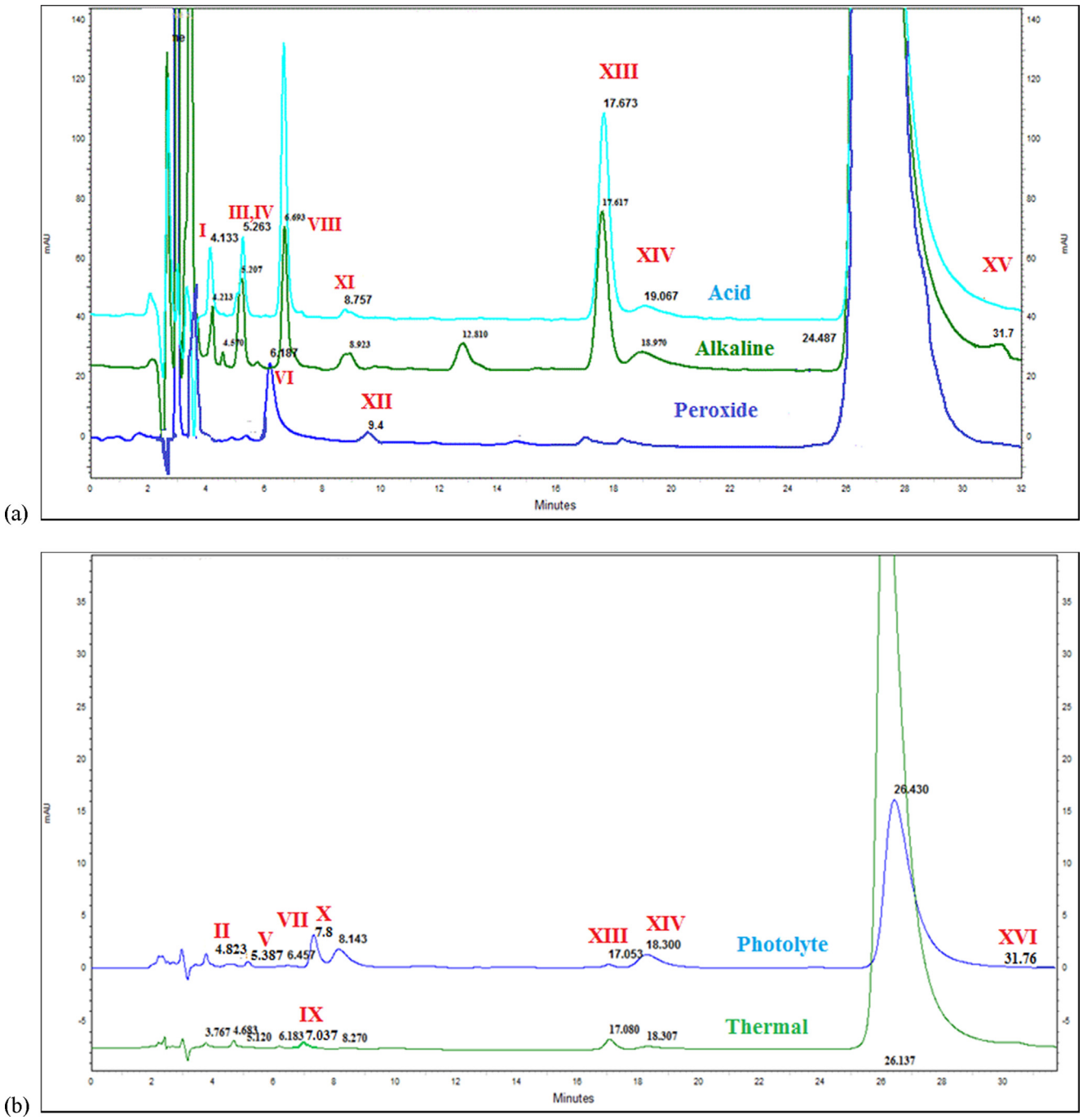

Fig. 1 Overlay chromatogram of AV (100 µg/mL) in (a) acid hydrolysis, alkaline hydrolysis and peroxide (b) photolytic and thermal degradation in the optimized chromatographic condition.

m/*z* 375.09 was formed due to the loss of $C_5H_7N_3$ (Diamino pyridine). Further, it fragments into MS^3 *m*/*z* 357.1 due to loss of H_2O (water) molecule and MS^4 *m*/*z* 342.00 was formed due to removal of the methyl group. Then AV fragments into MS^5 *m*/*z* 329.14 due to loss of - COH. At last due to cleavage of a single bond from *m*/*z* 329.14 structure it converted in to *m*/*z* 155.12. The MS/MS spectra reveals that *m*/*z* 155.12 is common to the last fragment of AV, having a molecular formula of C_8H_8ClO and chemical name of 2-chloro-1-methoxy-4-methyl-benzene. The best possible molecular formula and exact masses for the fragments were calculated as shown in Table 2.

3.3. Characterization of the impurities and degradation products using mass data

All the D.P.s were characterized based on LC-MS/MS. The line spectra of all the D.P.s were taken in ESI positive (ES+) mode. Accurate mass data of the molecular ions, their fragments, and accurate masses were listed in Table 2. Degradation peaks generated in all conditions were numbered as AV I to AV XVI and structures were predicted as shown in Fig. 3. They were characterized and identified from mass data. The

Table 1 Result from stress degradation study of AV.

Forced degradation condition	Stress degradation condition	% Appropriate degradation observed	% Mass balance obtained
Acid hydrolysis	1 N HCl at 60 °C for 9 hr	21.710	89
	1 N HCl at 70 °C for 8 hr	25.620	88
	1 N HCl at 80 °C for 6 hr	22.390	89
Alkaline hydrolysis	1 N NaOH at 60 °C for 4 hr	20.000	92
	1 N NaOH at 70 °C for 4 hr	23.550	91
	1 N NaOH at 80 °C for 3 hr	25.000	92
Neutral hydrolysis	60 °C for 12 hr	14.001	91
	70 °C for 12 hr	16.902	92
	80 °C for 12 hr	19.210	92
Oxidative hydrolysis	1% H_2O_2 for 4 hr	22.171	82
	6% H_2O_2 for 2 hr	30.521	82
	10% H_2O_2 for 30 min	16.250	83
Photolytic degradation	Solid-state 8 hr	22.391	98
	Liquid state 6 hr	23.000	98
	Solid sample at 1.2 million Lux hr for 6 hr in Photostability chamber	28.966	99
Thermal degradation	Solid-state, 60 °C for 7 hr	28.000	95
	Liquid state, 60 °C for 5 hr	28.501	96

data obtained in LC-MS and MS/MS studies were systematically utilized for the structure elucidation of D.P.s of AV as described below.

3.3.1. Acid degradation products

3.3.1.1. AV I (m/z 450.00) (a). The degradation product AV I, *m/z* 450 with an elemental composition $C_{22}H_{26}N_8O_3$ detected at 4.13 min in acid and alkaline hydrolysis conditions. LC-MSMS/MS line spectra of AV I in **Supplementary Fig S2 (i),** showed the formation of fragments with *m/z* 450.00, *m/z* 375.10, and *m/z* 343.15. Structure of AV I having –OH functional group, in the presence of hydrochloric acid and temperature, hydroxyl (–OH) functional group replaced with chlorine group (-Cl) and further water molecule removed. AV I (*m/z* 450) converted into *m/z* 468.94 due to chlorination. Further *m/z* 468.94 reduced to a fragment of *m/z* 375.10, indicating the loss of $C_4H_6N_4$. Lastly from the structure of *m/z* 375.10 removal of $–CH_3O$ and lead to formation of *m/z* 343.15. The product ion peaks at *m/z* 468, *m/z* 375, *m/z* 343, and *m/z* 155 indicates the presence of chlorine in structure. The elemental compositions of all these ions have been confirmed by mass measurements (Table 2, **Supplementary Fig S2 (i)**). Based on these data, AV I was identified as 4-{[(4-methoxyphenyl) methyl] amino} –2- [2-(hydroxymethyl) pyrrolidin-1-yl] - N-(pyrimidin-2-yl methyl) pyrimidine- 5- carboxamide.

AV III and IV are co-eluting peaks observed with LC and confirmed during LC-MS/MS study. They were named AV III (b) and AV IV (c) having a molecular weight of *m/z* 401.00 and *m/z* 358.08, respectively.

*3.3.1.2. **AV III (m/z 401.00) (b)**.* The degradation product AV III at *m/z* 401 with an elemental composition $C_{18}H_{17}ClN_6O_3$ detected at 5.26 min in acid and alkaline hydrolysis conditions. LC-MS/MS spectra as shown in **Supplementary Fig S2 (ii,b)**, showed the formation of fragments of AV III (b) (*m/z* 401) and *m/z* 358.08 (c). Further AV III fragmented into *m/z* 266.10 and *m/z* 155.04. The AV III (*m/z* 401) structure break from –CH bond and converted into $C_{12}H_{12}ClN_3O_2$ (*m/z* 266.10) due to loss of $C_6H_7N_3O$ (*m/z* 137.14). Lastly *m/z* 266.10 (b1) converted into two fragments of *m/z* 155.04 (C_8H_8ClO) and $C_4H_5N_3O$ (*m/z* 111.10). The diagnostic product ions at *m/z* 155 was common to the last fragment in each condition, having a molecular formula of C_8H_8ClO and chemical name of 2-chloro-1-methoxy-4-methyl-benzene. Based on these data (Table 2, **Supplementary Fig S2 (ii, b)** AV III was identified as 4-((3-chloro-4-methoxybenzyl) amino)-2-hydroxy-N-(pyrimidin-2-yl methyl) pyrimidine-5-carboxamide.

*3.3.1.3. **AV IV (m/z 358)(c)**.* The degradation product AV IV at *m/z* 358 with an elemental composition $C_{18}H_{22}N_5O_3$ detected at 5.26 min in acid and alkaline hydrolysis conditions. LC-MS/MS spectra as shown in **Supplementary Fig S2 (iii, c)**, showed that degradation product AV IV (*m/z* 358.08) (c) was co-eluting with AV III (*m/z* 401). From the AV IV (*m/z* 358.08 (c), $C_{18}H_{23}N_5O_3$) structure cleavage of –CH bond leads to formation of C_7H_7O (*m/z* 108.05) and $C_{11}H_{16}N_5O_2$ (*m/z* 249.13) (c1). Based on these data (Table 2, **Supplementary Fig S2 (iii, c)** AV IV was identified as 2-(2-(hydroxymethyl) pyrrolidin-1 -yl)-4-((4-methoxybenzyl) amino) pyrimidine –5-carboxamide.

*3.3.1.4. **AV VIII (m/z 393)(d)**.* The degradation product AV VIII at *m/z* 393 with an elemental composition $C_{18}H_{21}ClN_4O_4$ detected at 6.69 min in acid and alkaline hydrolysis conditions. An LC-MS/MS spectrum of AV VIII (*m/z* 393.17) (d) shows the presence of chlorine abundance (1:3) in mass spectra which confirms the presence of chlorine in structure as shown in **Supplementary Fig S2 (iv)**. The LC-MS/MS spectra showed the fragments of *m/z* 393.17, *m/z* 375.10 and *m/z* 155.06. AV VIII having a molecular formula of $C_{18}H_{20}ClN_4O_3$ converted into $C_{18}H_{20}ClN_4O_3$ (*m/z* 375.10) due to loss of 18 u which suggests loss of H_2O from the *m/z* 393.17 structure. Further *m/z* 375.10 fragmented into *m/z* 155.06 due to cleavage of –CH bond. The product ions at *m/z* 393, *m/z* 375, and *m/z* 155 act as diagnostic ions to propose the structure of AV VIII. Based on these data (Table 2, **Supplementary Fig S2 (iv)** AV VIII was identified as 4-{[(3-chloro-4-methoxy phenyl) methyl] amino}-2-[2-(hydroxymethyl) pyrrolidin-1-yl] pyrimidine-5-carboxylic acid. The Can, 2018 had identified AV VIII (*m/z* 393) as related substance 2, which formed due to replacement of the amide group with an acidic group.

*3.3.1.5. **AV XI (m/z 349.17)(e)**.* The acid and alkaline hydrolytic degradation product AV XI at *m/z* 349.17 with an elemental composition $C_{17}H_{21}ClN_4O_2$ detected at 8.75 min. The LC-MS/MS spectra shown in **Supplementary Fig S2 (v)** indicate peak having a molecular mass of *m/z* 349.17 (e). The mass difference between the AV XI (*m/z* 349.17) and product ion *m/z*

Table 2 Accurate mass data of molecules and their fragments.

No	[a]Peak name	[b]Peak code	[c]Degradation condition	[d]Rt (min)	[e]RRT	[f]MW	[g]Empirical formula	[h]MS/MS fragments
1	AV I	a	Acid, Alkaline	4.13	0.156	450	C_{22} H_{26} N_8 O_3	C_{22} H_{26} N_8 O_3 (450.00) C_{18} H_{22} Cl N_5 O_2 (375.10) C_{17} H_{19} Cl N_5 O (343.15)
2	AV II	i	Photolytic, Thermal	4.82	0.160	498	C_{23} H_{26} Cl N_7 O_4	C_{23} H_{26} Cl N_7 O_4 (498.00) C_{15} H_{19} N_7 O_3 (343.43) C_8 H_8 Cl O (155.03)
3	AV III	b	Acid, Alkaline	5.26	0.198	401	C_{18} H_{17} Cl N_6 O_3	C_{18} H_{17} Cl N_6 O_3 (401.82) C_{12} H_{12} Cl N_3 O_2 (266.10) C_6 H_7 N_3 O (137.14) C_8 H_8 Cl O (155.04) C_4 H_5 N_3 O (111.10)
4	AV IV	c	Acid, Alkaline	5.26	0.198	358	C_{18} H_{22} N_5 O_3	C_{18} H_{22} N_5 O_3 (358.08) C_{11} H_{16} N_5 O_2 (249.13) C_7 H_7 O (108.05)
5	AV V	j	Photolytic, Thermal	5.39	0.201	500	C_{23} H_{26} Cl N_7 O_4	C_{23} H_{26} Cl N_7 O_4 (500) C_{23} H_{25} Cl N_7 O_3 (482.20) C_8 H_8 Cl O (155.036)
6	AV VI	o	Oxidative	6.19	0.233	518	C_{23} H_{25} Cl_2 N_7 O_3	C_{23} H_{25} Cl_2 N_7 O_3 (518.25) C_{17} H_{19} Cl_2 N_4 O_2 (381.05) C_8 H_8 Cl O (155.13)
7	AV VII	k	Photolytic, Thermal	6.46	0.245	515	C_{23} H_{26} Cl N_7 O_5	C_{23} H_{26} Cl N_7 O_5 (515.92) C_{23} H_{27} N_7 O_5 (482.18)
8	AV VIII	d	Acid, Alkaline	6.69	0.251	393	C_{18} H_{21} Cl N_4 O_4	C_{18} H_{21} Cl N_4 O_4 (393.17) C_{18} H_{20} Cl N_4 O_3 (375.10) C_8 H_8 Cl O (155.06)
9	AV IX	n	Thermal	7.04	0.282	454	C_{22} H_{24} Cl N_7O_2	C_{22} H_{24} Cl N_7O_2 (454.17) C_{17} H_{18} Cl N_4 O_2 (345.10) C_5 H_7 N_3 (109.13)
10	AV X	l	Photolytic	7.85	0.286	468	C_{22} H_{24} Cl N_7 O_3	C_{22} H_{24} Cl N_7 O_3 (468.98) C_{15} H_{18} N_6 O_2 (312.25) C_7 H_6 Cl N O (155.04)
11	AV XI	e	Acid, Alkaline	8.75	0.330	349.17	C_{17} H_{21} Cl N_4 O_2	C_{17} H_{21} Cl N_4 O_2 (349.17) C_{17} H_{20} Cl N_4 O (331.10) C_9 H_{13} N_4 (178.24) C_8 H_8 Cl O (155.04)
12	AV XII	p	Oxidative	9.40	0.355	488	C_{23} H_{30} Cl N_7 O_3	C_{23} H_{30} Cl N_7 O_3 (488.17) C_8 H_8 Cl O (155.03) C_{15} H_{23} N_7 O_2 (333.39)
13	AV XIII	f	(Acid, Alkaline, Thermal, Oxidative, Photolytic)	17.67	0.665	450	C_{22} H_{26} N_8 O_3	C_{22} H_{26} N_8 O_3 (450.25) C_{18} H_{21} N_4 O_3 (341.13) C_{17} H_{19} N_4 O_3 (328.17) C_5 H_7 N_3 (109.13)
14	AV XIV	g	(Acid, Alkaline, Thermal, Oxidative, Photolytic)	19.06	0.718	392	C_{18} H_{22} Cl N_5 O_3	C_{18} H_{22} Cl N_5 O_3 (392.17) C_{18} H_{20} Cl N_4 O_3 (375.13) C_8 H_8 Cl O (155.09)
15	AV XV	h	Alkaline	31.70	1.195	526.17	C_{25} H_{27} Cl N_8 O_3	C_{25} H_{27} Cl N_8 O_3 (526.17) C_{20} H_{22} Cl N_5 O_3 (417.07) C_5 H_6 N_3 (109.13)
16	AV XVI	m	Photolytic	31.76	1.197	485.15	C_{23} H_{26} Cl N_7 O_3	C_{23} H_{26} Cl N_7 O_3 (485.83) C_{18} H_{21} Cl N_4O_3 (376.15) C_{18} H_{20} Cl N_4O_2 (359.83) C_{17} H_{20} Cl N_4O (328.36) C_8 H_8 Cl O (155.08)

[a] Peak name refers to the RRT of AV degradation peaks found during different degradation conditions.
[b] Peak code refers to the degradation condition wise numbering of AV degradation peaks.
[c] Degradation condition refers to Coded peak present in different degradation conditions.
[d] Rt refers to rention time in minute for degradation peaks.
[e] RRT refers to relative rention time for degradation peaks in different conditions.
[f] MW refers to molecular weight of degradation products.
[g] Empirical formula refers to chemical composition of degradation products.
[h] MS/MS fragments refers to the mass fragmentation pattern found from LC-MS/MS

331.10 ($C_{17}H_{20}ClN_4O$) was 18 u which suggests that *m/z* 331 form by loss of H_2O from the AV XI. Structure of *m/z* 331.10 further converted into C_8H_8ClO (*m/z* 155.04) and $C_9H_{13}N_4$ (*m/z* 178.24) due to cleavage of –CH bond. The product ions at *m/z* 349, *m/z* 331, and *m/z* 155 are diagnostic ions for the proposed structure of AV XI. Based on these data (Table 2, **Supplementary Fig S2 (v)** AV VIII was identified as (1-(4-((3-chloro-4-methoxybenzyl) amino) pyrimidin-2-yl) pyrrolidin-2-yl) methanol.

*3.3.1.6. **AV XIII (m/z 450.25)(f)***. The acid, alkaline hydrolysis, thermal, oxidative, and photolytic degradation product AV XIII (*m/z* 450.25) with an elemental composition $C_{22}H_{26}N_8O_3$ detected at 17.67 min. LC-MS/MS spectra of AV XIII *(m/z 450.25)* (f) as shown in **Supplementary Fig S2 (vi)**. AV XIII having the same molecular mass as AV I but having different product ion due to *R* form enantiomer. The LC-MS/MS spectra show peaks of *m/z* 450.25, *m/z* 341.13, and *m/z* 328.17. AV XIII (*m/z* 450.25) fragmented into *m/z* 341.13 due to the removal of $C_5H_7N_3$ (*m/z* 109.13). Obtained *m/z* 341.13 converted into $C_{17}H_{19}N_4O_3$ (*m/z* 328.17) due to the loss of the methyl ($–CH_3$) group from the structure. The product ions at *m/z* 450.25, *m/z* 341.13, and *m/z* 328.17 were diagnostic ions for the proposed structure of AV XIII. Based on these data (Table 2, **Supplementary Fig S2 (vi)** AV XIII was identified as 2-(2-(hydroxymethyl) pyrrolidin-1-yl) – 4 - ((4-methoxybenzyl) amino)- N -(pyrimidin – 2-yl methyl) pyrimidine – 5-carboxamide.

*3.3.1.7. **AV XIV (m/z 392.17)(g)***. The degradation product AV XIV at *m/z* 392 with an elemental composition $C_{18}H_{22}ClN_5O_3$ detected at 19.06 min in acid hydrolysis, alkaline hydrolysis, thermal, oxidative and photolytic degradation conditions. LC-MS/MS spectra of AV XIV (*m/z* 392.17) (g) as shown in **Supplementary Fig S2 (vii)**. The spectra showed the product ion peak at *m/z* 392.17, *m/z* 375.13, and *m/z* 155.09. The LC-MS/MS spectra of AV XIV showed a high abundance product ion at *m/z* 392.17, which fragmented into *m/z* 375.13 due to the removal of ammonia (NH_3) from structure. Further *m/z* 375.13 fragmented into *m/z* 155.09 and *m/z* 222.24 due to cleavage of –CH bond. Based on these data (Table 2, **Supplementary Fig S2 (vii)** AV XIV was identified as 4-((3-chloro-4-methoxybenzyl) amino)-2-(2-(hydroxymethyl) pyrrolidin-1-yl) pyrimidine –5 - carboxamide. The Can, 2018 had identified AV XIV (*m/z* 393) as related substance 1, which formed due to electro withdrawing properties of the amide moiety.

3.3.2. Alkaline degradation products

The degradation pattern of alkaline degradation conditions was similar to the acidic condition. In alkaline degradation, all the D.P.s of acid degradation were found. In addition to that one more D.P. was found having molecular weight as *m/z* 526.17.

*3.3.2.1. **AV XV (m/z 526.17)(h)***. The base hydrolytic degradation product AV XV at *m/z* 526.17 with an elemental composition $C_{25}H_{27}ClN_8O_3^+$ was detected at 31.70 min. During alkaline hydrolysis acetonitrile was used as solvent to solubilize AV in alkaline medium, hence degradation product AV XV (*m/z* 526.17) (h) formed due to addition of methyl cyanide (C_2H_3N, *m/z* 41.053) in AV structure. Acetonitrile adduct formation was further confirmed by using methanol as a solvent in place of acetonitrile and peak was absent. As shown in **Supplementary Fig S3**, *m/z* 526.17 further fragmented into $C_{18}H_{21}N_4O_3$ (*m/z* 417.07) due to the removal of $C_5H_6N_3$ (*m/z* 109.136). Based on these data (Table 2, **Supplementary Fig S3**, AV XV was identified as acetonitrile adduct of AV.

3.3.3. Photolytic degradation products

In photolytic degradation D.P.s II, V, VII, X, XIII, XIV, and XVI were found. From that D.P.s XIII and XIV were common for all degradation. Found new degradation products for photolytic degradation were D.P.s II, V, VII, X, and XVI.

*3.3.3.1. **AV II (m/z 498) (i)***. The photolytic and thermal degradation product AV II at *m/z* 498 with an elemental composition $C_{23}H_{26}ClN_7O_4$ detected at 4.82 min. The LC-MS/MS spectra of AV II (*m/z* 498.00) (i) show a higher abundance product ion peak at *m/z* 498.00 and further fragmented into *m/z* 155.07 as shown in **Supplementary Fig S4 (i)**. AV II converted into *m/z* 155.038 (C_8H_8ClO) and *m/z* 345.15 ($C_{15}H_{19}N_7O_3$) due to the breakage of - CH bond from the amino functional group. Based on these data of product ions (Table 2, **Supplementary Fig S4 (i),** AV II was identified as 4-((3-chloro-4-methoxybenzyl) amino)-2-(4-hydroxy-2-(hydroxymethyl) pyrrolidin-1-yl)-N-(pyrimidin-2-yl methyl) pyrimidine – 5 - carboxamide

*3.3.3.2. **AV V (m/z 500.00) (j)***. The photolytic and thermal degradation product AV V at *m/z* 500 with an elemental composition $C_{23}H_{26}ClN_7O_4$ detected at 5.39 min. *AV V* differs from *AV II* due to a change in the position of the hydroxyl (–OH) functional group. The LC-MS/MS spectra of AV V (*m/z* 500) (j) shows a high abundance product ion peak at *m/z* 500, *m/z* 482.20 and *m/z* 155.03 as shown in **Supplementary Fig S4 (ii).** From the structure of AV V (*m/z* 500) removal of the hydroxide group (–OH), it converted into *m/z* 482.20 having an elemental composition of $C_{23}H_{25}ClN_7O_3$. Further *m/z* 482.20 fragmented into *m/z* 155.03 and *m/z* 329.36 due to cleavage of –CH bond. Based on these data of product ions (Table 2, **Supplementary Fig S4 (ii))** structure of AV V was proposed and identified as 4-((3-chloro-4-methoxybenzyl) amino)-2-(2-hydroxy-5-(hydroxymethyl) pyrrolidin-1-yl)- N-(pyrimidin-2-yl methyl) pyrimidine-5-carboxamide.

*3.3.3.3. **AV VII (m/z 515)(k)***. The photolytic and thermal degradation product AV VII at *m/z* 515.92 with an elemental composition $C_{23}H_{26}ClN_7O_5$ detected at 6.46 min. The increase of 32 Da in molecular weight compared to the drug suggests that AV VII was a di-oxidative degradation product. The LC-MS/MS spectra of AV VII (*m/z* 515) (k) as shown in **Supplementary Fig S4 (iii)** indicates **the** presence of product ion peaks at *m/z* 515.92, *m/z* 482.18 and *m/z* 433. AV VII (*m/z* 515.92) converted into *m/z* 482.18 due to dechlorination (removal of -Cl group having a molecular mass of *m/z* 35). Further *m/z* 482.18 fragmented into *m/z* 433 ($C_{22}H_{24}N_7O_3$) by removal of CH_2O_2 (*m/z* 45). Based on these data of product ions (Table 2, **Supplementary Fig S4 (iii))** structure of AV VII was proposed and identified as 3-((4-((3-chloro-4-methoxybenzyl) amino)-5-((pyrimidin-2-yl methyl) carbamoyl) pyrimidin-2-yl) (2-hydroxyethyl) amino) propanoic acid.

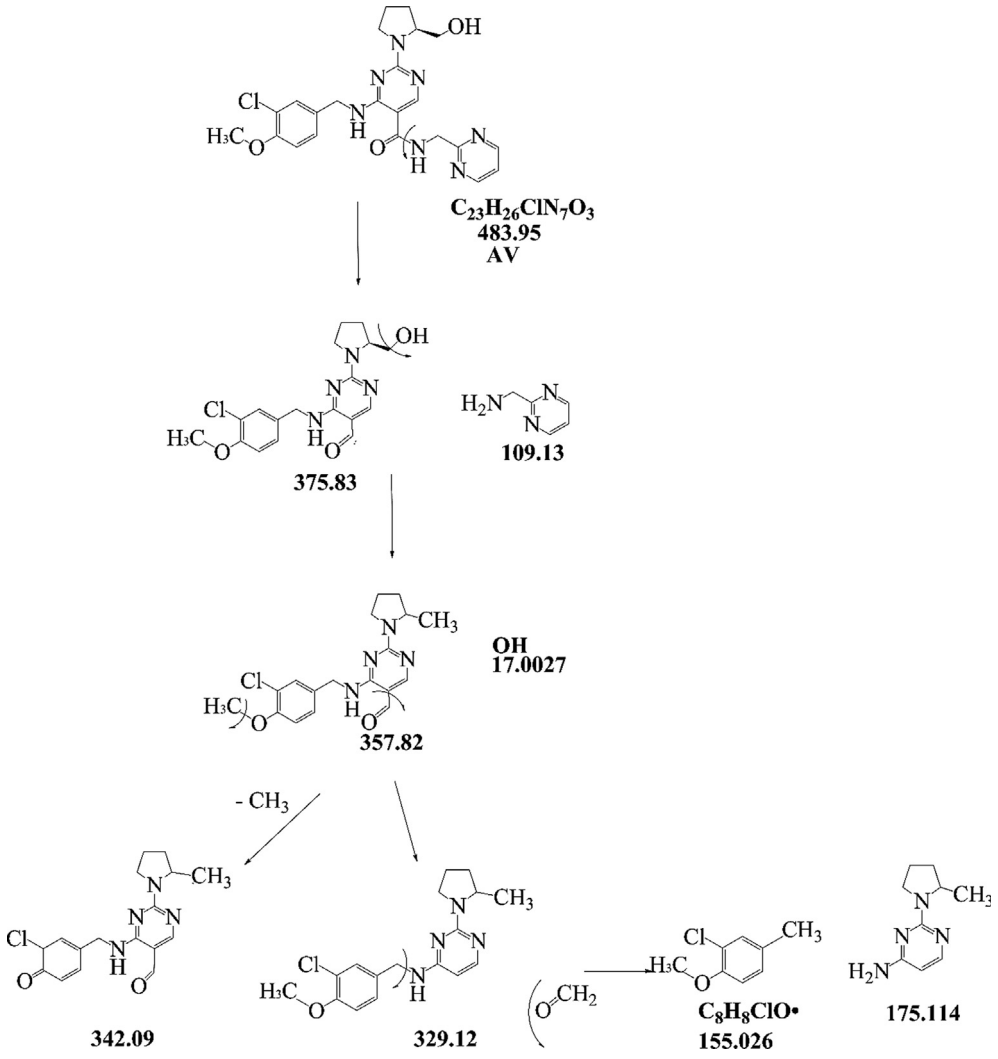

Fig. 2 Proposed fragmentation pattern of AV.

*3.3.3.4. **AV X (m/z 468.08) (l)***. The degradation product AV X at *m/z* 468 with elemental composition $C_{22}H_{24}ClN_7O_3$ detected at 7.85 min in photolytic degradation. The LC-MS/MS spectra of AV X (*m/z* 468.08) (l) having high abundance product ion peaks at *m/z* 468.08, *m/z* 312.25 and *m/z* 155.04 as shown in **Supplementary Fig S4 (iv)**. AV X (*m/z* 468.08) fragmented in to C_7H_6ClNO (*m/z* 155.04) and $C_{15}H_{17}N_6O_2$ (*m/z* 312.34) due to –CH bond cleavage. Based on product ions and fragment ions AV X structure was proposed as a demethylated analog of AV as shown in Table 2**, Supplementary Fig S4 (iv).** The Structure was identified as 4-((3-chloro-4-hydroxy benzyl) amino)-2-(2-(hydroxymethyl) pyrrolidin-1-yl) - N - (pyrimidin-2-yl methyl) pyrimidine-5-carboxamide.

3.3.3.5. AV XVI (m/z 485.83) (m). The degradation product AV XVI at *m/z* 485.83 with elemental composition $C_{23}H_{26}ClN_7O_3$ detected at 31.76 min in photolytic degradation. The LC-MS/MS spectra of AV XVI (*m/z* 485.83 (m) showed high abundance product ions at *m/z* 485.83, *m/z* 468.08, *m/z* 376.15, *m/z* 328.36 and *m/z* 155.08 as shown in **Supplementary Fig S4 (v)**. The structure of AV XVI (*m/z* 485.83) converted into product ion at *m/z* 376.15 due to the removal of $C_5H_7N_3$ (aminomethyl pyrimidine). Further from the structure of *m/z* 376.15 loss of hydroxide group and $–CH_2O$ group, it converted into product ion at *m/z* 328.36. Lastly *m/z* 328.36 product ion peak fragmented into *m/z* 155.08 (C_8H_8ClO) and *m/z* 177.23. Based on data of product ion peaks and fragmentation pattern as shown in Table 2**, Supplementary Fig S4 (v)** structure of AV XVI was proposed and identified as a 4-((3-chloro-4-methoxybenzyl) amino) – 2- (2- (hydroxymethyl) pyrrolidin-1-yl) – N - (pyrimidine – 2- yl-methyl) pyrimidine-5- carboxamide.

3.3.4. Thermal degradation products

During thermal degradation D.P.s II, V, IX, XIII and XIV were found. Common D.P. between photolytic and thermal degradation was D.P. II. Further D.P.s XIII and XIV were common for all degradation. For thermal degradation conditions found different D.P. was IX.

*3.3.4.1. **AV IX (m/z 454) (n)***. The degradation product AV IX at *m/z* 454.17 with an elemental composition $C_{22}H_{24}ClN_7O_2$ was detected at 7.04 min in thermal condition. The LC-MS/MS spectra of AV IX (*m/z* 454) (n) showed a high abundance peak at *m/z* 454.17 and *m/z* 345.10 as shown in **Supplementary**

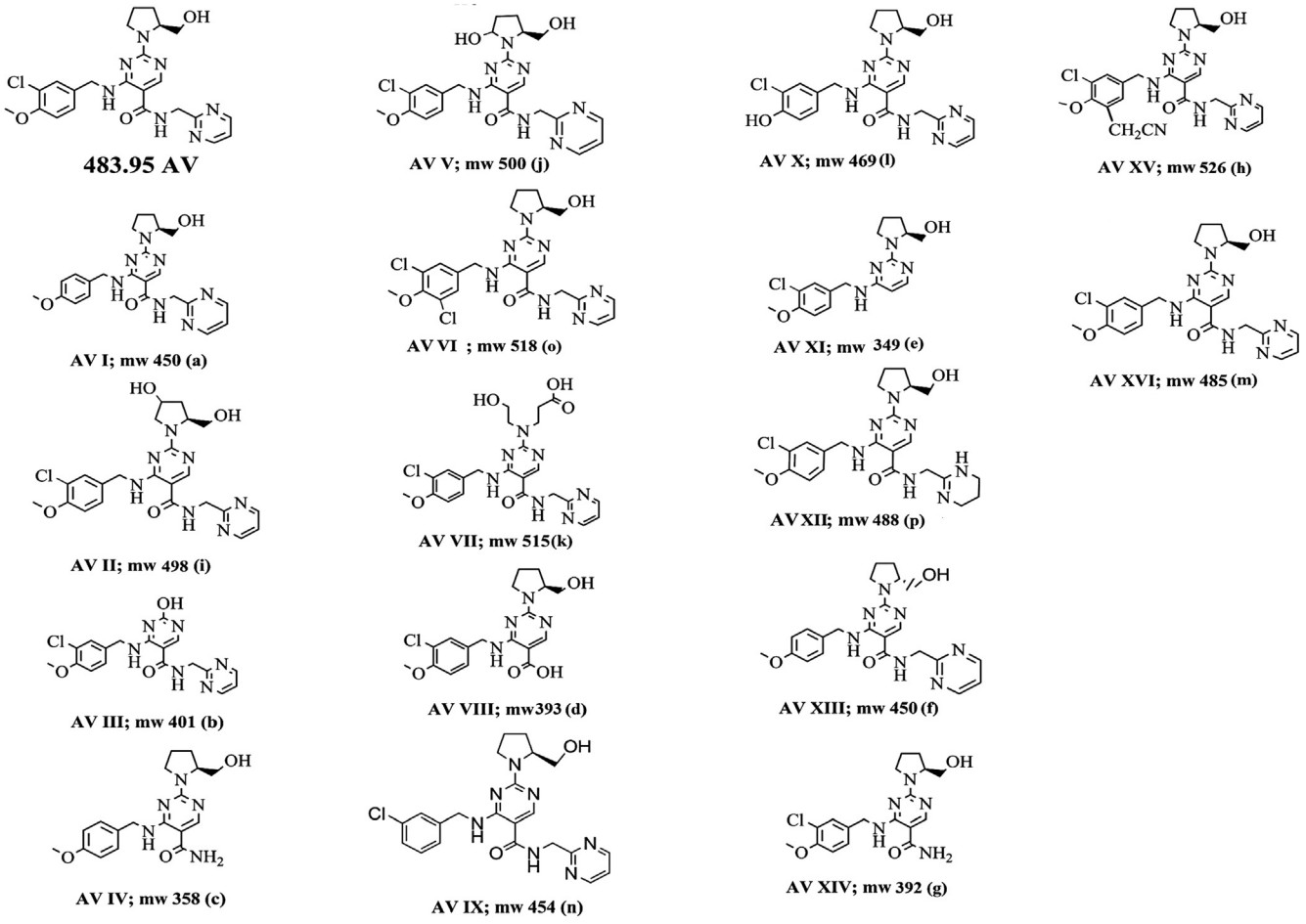

Fig. 3 Structure of AV and proposed structures of its degradation products.

Fig S5. AV IX (*m*/*z* 454) fragmented in to $C_{17}H_{18}ClN_4O_2$ (*m*/*z* 345.8) due to removal of $C_5H_7N_3$ (*m*/*z* 109.13). Based on data of product ion peak and fragmentation pattern as shown in Table 2, **Supplementary Fig S5** structure of AV XVI was proposed and identified as 4-((3-chlorobenzyl) amino) −2- (2- (hydroxymethyl) pyrrolidin − 1- yl) - N -(pyrimidin – 2 –yl methyl) pyrimidine −5- carboxamide, which is the demethoxybenzyl analog of AV.

3.3.5. Oxidative degradation products

Found D.P.s in oxidative conditions were VI, XII, XIII and XIV. D.P.s XIII and XIV were common for acid, alkaline, oxidative, photolytic and thermal degradation. Found new D.P.s in oxidative conditions were VI and XII.

3.3.5.1. ***AV VI (m/z 518.25) (o)***. The oxidative degradation product AV VI at *m*/*z* 518.25 with an elemental composition $C_{23}H_{25}Cl_2N_7O_3$ was detected at 6.19 min. The LC-MS/MS spectra of AV VI (*m*/*z* 518.25) (o) was as shown in **Supplementary Fig S6 (i).** The spectra showed high abundance product ions at *m*/*z* 534.17 (addition of oxygen in *m*/*z* 518.25), *m*/*z* 518.25 (M + 16 peak, the addition of one chlorine functional group in the structure of AV), *m*/*z* 381.05 (removal of $C_6H_6N_3O$ from *m*/*z* 518.25) and *m*/*z* 155.13. The *m*/*z* 381.05 fragmented into *m*/*z* 155.03 (last most common fragment) and *m*/*z* 193.109 due to cleavage of –CH bond. Based on data of product ion peaks and fragmentation pattern as shown in Table 2, **Supplementary Fig S6 (i)** structure of AV VI was proposed and identified as 4-((3,5-dichloro-4-methoxybenzyl) amino) – 2- (2-(hydroxymethyl) pyrrolidin-1-yl) – N -(pyrimidin-2-yl methyl) pyrimidine −5- carboxamide.

3.3.5.2. ***AV XII (m/z 488.17) (p)***. The oxidative degradation product AV XII at *m*/*z* 488.17 with an elemental composition $C_{23}H_{30}ClN_7O_3$ was detected at 9.40 min. The LC-MS/MS spectra of AV XII (*m*/*z* 488.17) (p) was as shown in **Supplementary Fig S6 (ii).** The spectra showed high abundance product ions at *m*/*z* 488.17 (conversion of a pyrimidine to tetrahydro pyrimidone in AV due to oxidation), *m*/*z* 333.39 (fragment due to cleavage of –CH bond from *m*/*z* 488.17) and *m*/*z* 155.03. Based on data of product ions and fragmentation pattern as shown in Table 2, **Supplementary Fig S6 (ii)** structure of AV XII was proposed and identified as 4-((3-chloro-4-methoxybenzyl) amino)-2-(2-(hydroxymethyl) pyrrolidin-1-yl) – N -((1,4,5,6 – tetrahydro pyrimidine – 2 -yl) methyl) pyrimidine-5-carboxamide.

3.4. Postulated mechanistic pathway for the formation of D.P.s

Based on the data obtained from the line spectra of LC-MS/MS studies of each degradation product, the proposed degradation pathway of AV in different degradation conditions

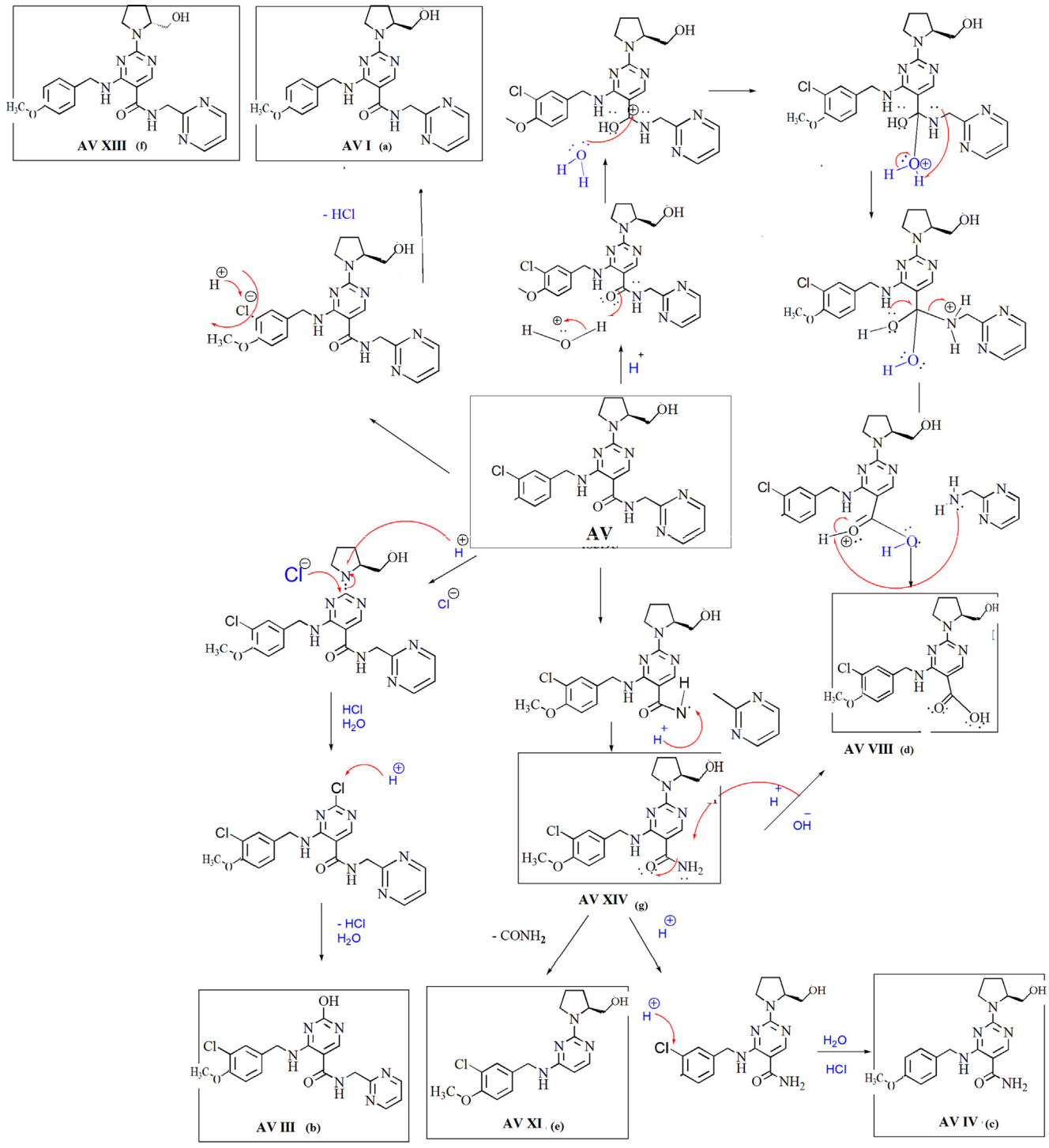

Fig. 4 Degradation mechanism of AV in acidic condition.

were established. The degradation pathways for AV in (i) acid, (ii) alkaline, (iii) photolytic, (iv) thermal and (v) oxidative degradation conditions were shown as Fig. 4, Fig. 5, Fig. 6, Fig. 7 **and** Fig. 8**.**

In acid hydrolysis, AV XIV form due to cleavage of –CH bond between carbonyl amide and pyrimidine ring from the structure of AV. Formation of AV VIII from the structure of AV explained by nucleophilic substitution reaction and formation of aryl carboxylic acid from aryl amide with loss of amino pyrimidine. From the AV XIV structure loss of 'CONH' functional group leads to the formation of the AV XI degradation product. AV IV degradation product form due to dechlorination from the structure of AV XI. AV III degradation product form in the presence of acid hydrolysis by removal of pyrrolidine ring by – OH (hydroxy) functional group. Formation of AV I and AV XIII can be explained by

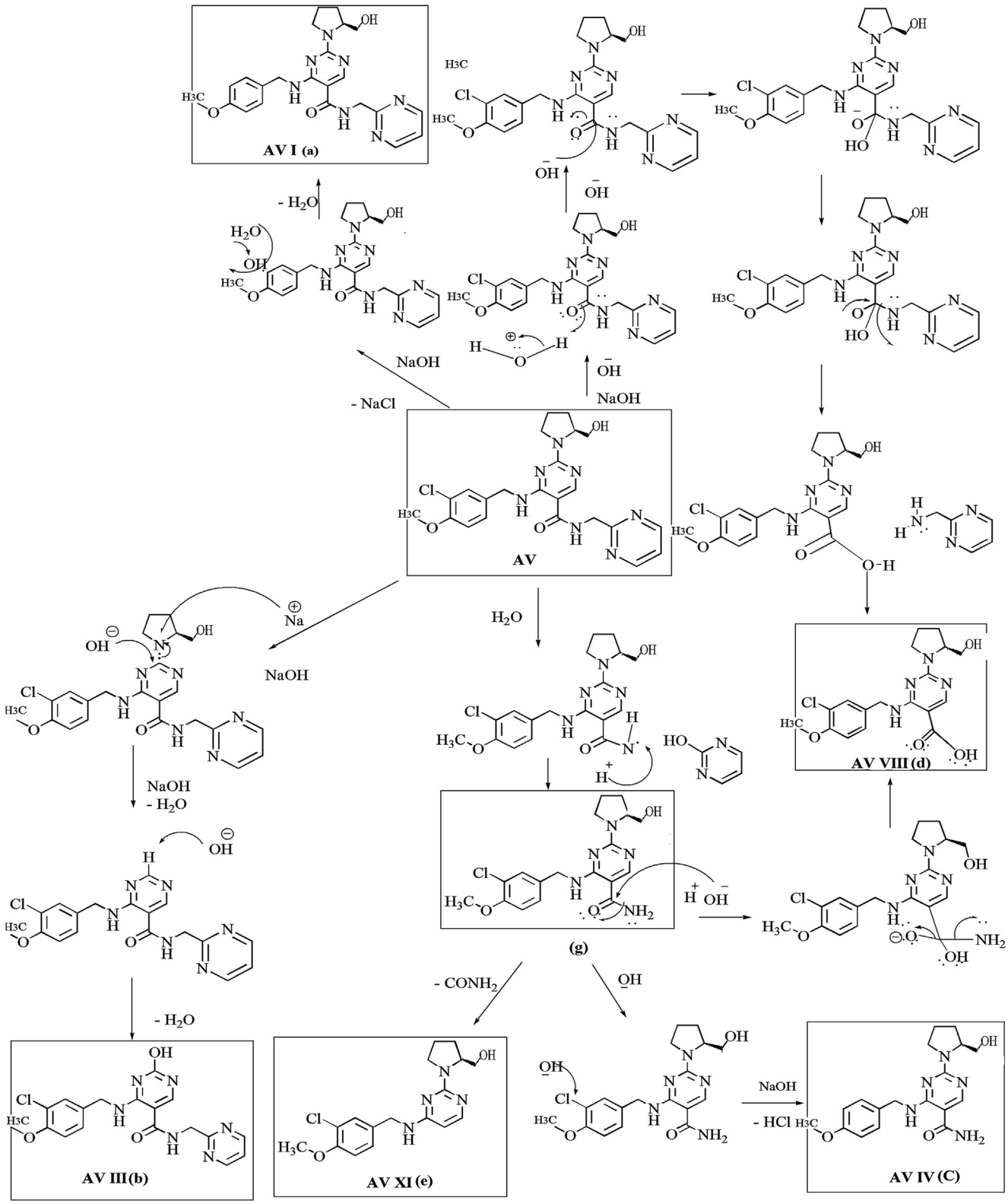

Fig. 5 Degradation mechanism of AV in alkaline condition.

dechlorination from the AV structure. Both degradation product having the same molecular mass but position of - OH functional group is different and further fragments are different, confirms that AV XIII is R isomeric form of AV I. (Fig. 4)

In the case of alkaline hydrolysis, the formation of AV I from AV can be explained by the removal of chlorine functional group. The formation of AV VIII is explained by nucleophilic substitution reaction due to OH^- ion abstracts the

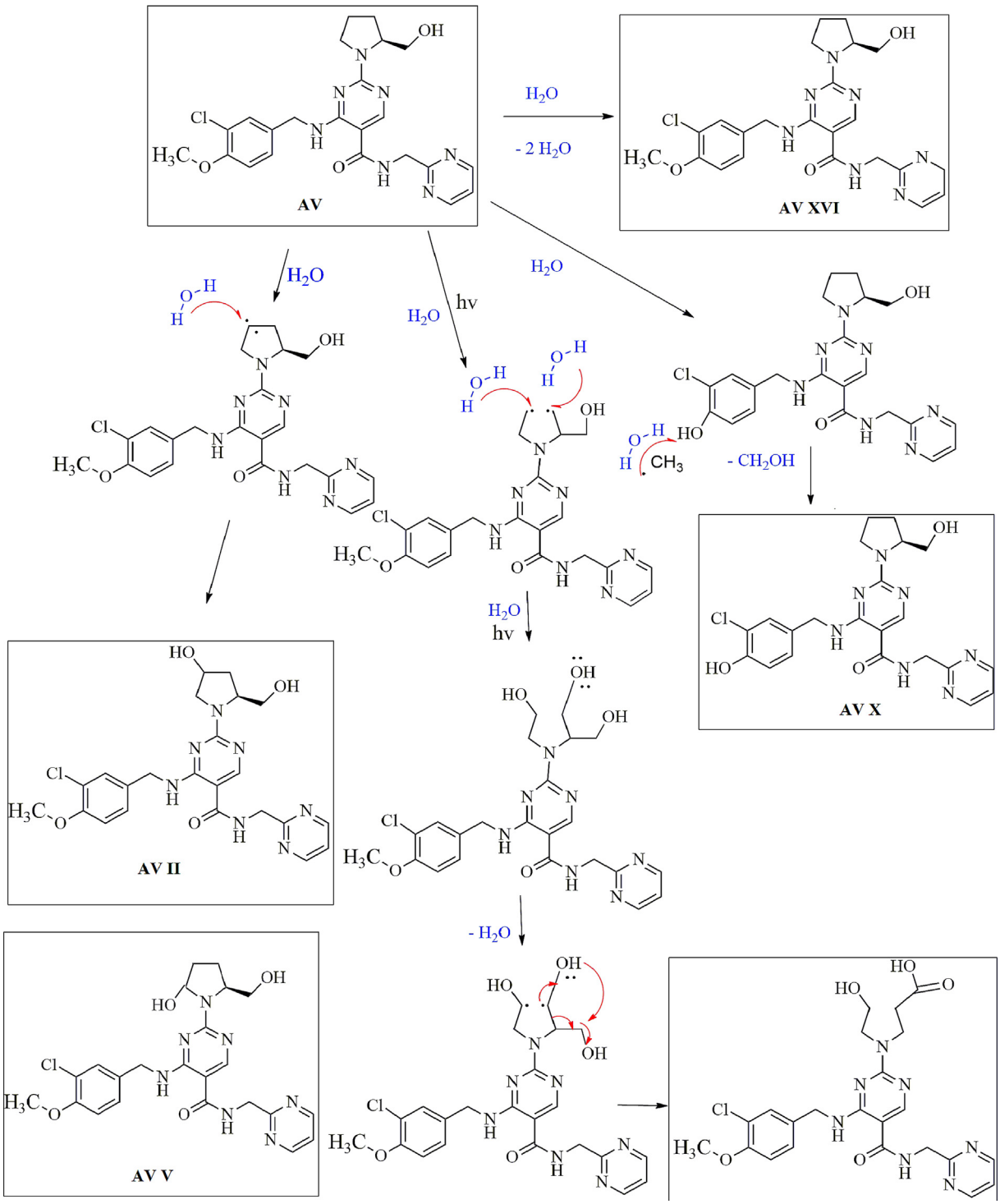

Fig. 6 Degradation mechanism of AV in photolytic condition.

proton followed by hydrolysis. AV XIV form due to hydrolysis of AV and removal of the pyrimidine ring. The formation of AV XI is explained by the removal of 'CONH' functional group from the structure of AV and AV IV is due to dechlorination from the structure XIV. AV XV is identified as acetonitrile adduct formation with AV (Fig. 5).

In the case of photolytic degradation condition formation of AV related substance is identified as AV XVI, due to the presence of free radical and hydrolysis. AV X formation can explained by demethylation from the AV structure. The formation of AV VII can explained by the opening of the pyrrolidine ring in the presence of free radical and further attachment of

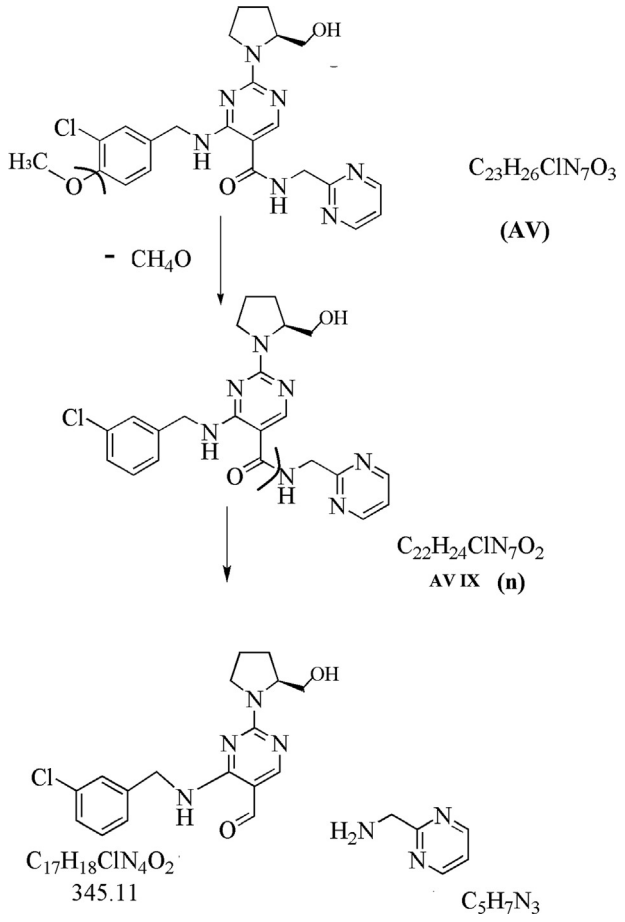

Fig. 7 Degradation mechanism of AV in thermal condition.

the hydroxyl functional group on it, which involved a radical cation mechanism. AV V and AV II form due to attachment of - OH functional group in the AV structure (Fig. 6).

In the case of thermal hydrolysis, AV IX formation can explained by the removal of dimethoxy benzyl from the AV structure due to energy and bond cleavage (Fig. 7).

In oxidative degradation formation of AV XII is due to oxidation by peroxide and AV VI is due to the addition of chlorine functional group in AV structure (Fig. 8).

3.5. In silico studies

In silico physicochemical parameters and toxicity risk assessment study (prediction) was carried out to get an idea about the physicochemical properties and any probable toxicity due to the impurities. Factors of toxicity risk assessment like mutagenicity, tumorigenicity, irritant and reproductive effects (Table 3) relies on a computed set of structural fragment that give rise to toxicity alerts in case they are encountered in the structure of impurity. These fragment lists were created by rigorously shredding all compounds of the RTECS database known to be active in a certain toxicity class (e.g. mutagenicity). During the shredding, any impurity was first cut at every rotatable bond leading to a set of core fragments. These in turn were used to reconstruct all possible bigger fragments being a substructure of the original impurity. Afterward, a substructure search process determined the occurrence frequency of any fragment (core and constructed fragments) within all compounds of that toxicity class. It also determined these fragment's frequencies within the structures of more than 3000 traded drugs. Toxicity risk alerts are an indication that the impurity may be harmful concerning the risk category specified (toxic, moderately toxic, and non-toxic). Results of toxicity prediction study revealed that no impurity is at any risk of tox-

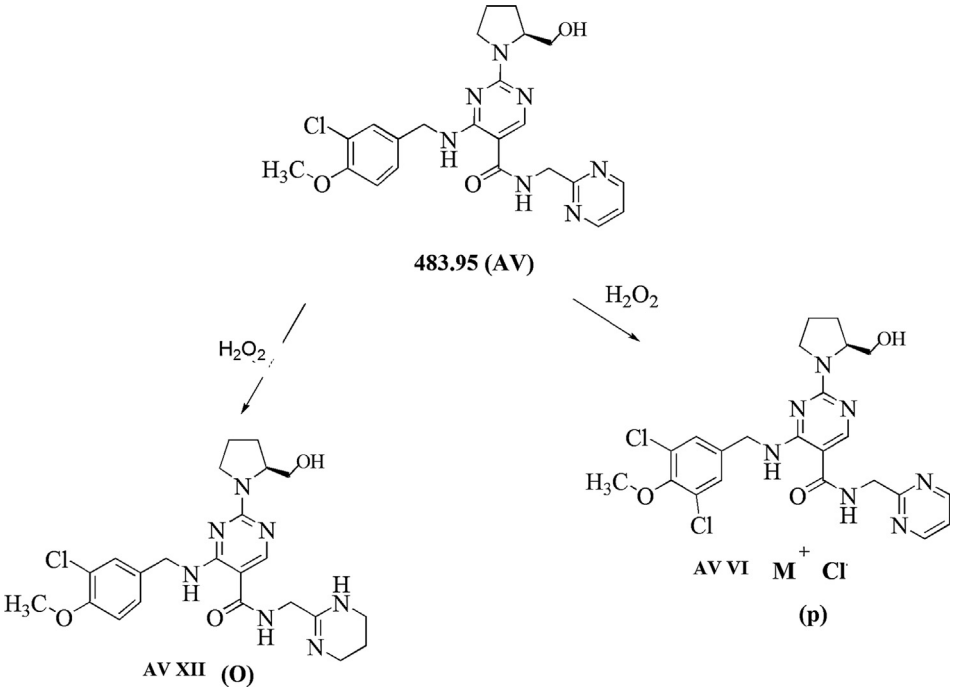

Fig. 8 Degradation mechanism of AV in oxidative condition.

Table 3 In Silico toxicity studies for AV and degradation products.

Structures of impurity	Toxicity risk assessment study				Physicochemical parameters			
	[a]Mutagenicity	[b]Tumorigenicity	[c]Irritating effect	[d]Reproductive effect	[e]cLogp	[f]Solubility (LogS)	[g]TPSA	Mol. wt
AV	–	–	–	–	1.49	−3.75	125.3	483.95
AV I (a)	–	–	–	–	0.88	−3.01	125.3	450
AV II (i)	–	–	–	–	0.64	−3.35	145.6	498
AV III (b)	–	–	–	–	1.26	−2.86	122.1	401
AV IV (c)	–	–	–	–	0.79	−3.49	113.6	358
AV V (j)	–	–	–	–	1.14	−3.56	145.6	500
AV VI (o)	–	–	–	–	2.1	−4.48	125.3	518
AV VII (k)	–	–	–	–	0.56	−3.03	162.6	515
AV VIII (d)	–	–	–	–	1.79	−4.15	107.8	393
AV IX (n)	–	–	–	–	1.56	−3.73	116.1	454
AV X (l)	–	–	–	–	1.21	−3.43	136.3	469
AV XI (e)	–	–	–	–	2.31	−4.41	70.51	349
AV XII (p)	–	–	–	–	1.13	−4.38	124	488
AV XIII (f)	–	–	–	–	0.88	−3.01	125.3	450
AV XIV (g)	–	–	–	–	1.39	−4.23	113.6	392
AV XV (h)	–	–	–	–	1.5	−4.4	149.1	526
AV XVI (m)	–	–	–	–	1.49	−3.75	125.3	485

[a] Mutagenicity refers to the induction of permanent transmissible changes in the structure of the genetic material of cells or organisms.
[b] Tumorigenicity is the process by which neoplastic cells grow in tissue culture form tumors.
[c] Irritant may refer to a stimulus from a compound which causes irritation.
[d] Reproductive effective refers adverse effect of compounds that interferes with the reproductive organs of an organism, such as genitalia and gonads.
[e] The cLogP value of a impurity is a logarithm of its partition coefficient between n-octanol and water log(coctanol/cwater).
[f] Solubility (LogS): It is estimated logS value, and it is a unit stripped logarithm (base 10) of the solubility measured in mol/liter.
[g] Topological polar surface area (TPSA) of a impurity is the surface sum over all polar atoms or impurity, primarily oxygen and nitrogen, also including their attached hydrogen atoms.

icity. Prediction of physicochemical properties revealed that all the physicochemical parameters of impurities were within the acceptable limit.

Table 4 (i) Summary of validation parameter of SIAM of AV.

Parameter	AV
Detection wavelength (nm)	239
Linearity (μg/mL)	10–70
Regression coefficient (r^2)	0.997
Regression equation	y = 1E + 06x − 3E + 06
LOD (μg/mL)	0.360
LOQ (μg/mL)	1.150
Intraday precision % RSD (n = 3)	0.326 – 0.697
Interday precision % RSD (n = 3)	1.680 – 1.800
% Assay ± RSD (n = 6)	(99.430–102.040) ± 0.997
% Recovery ± RSD (n = 3)	99.280 ± 0.239–101.420 ± 0.092

(ii) System suitability parameters of stability method

Parameter	Observation	RSD[a]
Rt (mL/min)	27.160	0.450
Area (mAU)	13,026,886	0.680
Theoretical plate	9226	0.520
Tailing factor	1.270	0.550

[a] = Mean of five replicates.

3.6. *Method validation* (*ICH, 2005b*)

The developed stability-indicating method was validated as per ICH guidelines Q2 (R1) and results shown as per Table 4 **(i).** The system suitability of the developed method was checked for 10 μg mL^{-1} by evaluating % RSD values of peak area, asymmetry, theoretical plate, and retention time of five standard replicates. % RSD values were found less than 2, for all parameters as shown in Table 4 **(ii).** The regression coefficient was found to be 0.9970 for AV in the range of 10–70 μg mL^{-1} which confirms the linearity of the method. All degradation product peaks having resolution (>2) and peak purity from 0.990 – 0.999 indicating peaks were well separated. LOD and LOQ values were found to be 0.36 μg mL^{-1} and 1.15 μg mL^{-1}, respectively. The interday and intraday precision was evaluated at three different concentrations, i.e. 10, 30, and 50 μg mL^{-1} (each in triplicate) on consecutive three days and the same day respectively. The % RSD values for interday and intraday was found to be 1.680–1.800 and 0.326–0.697, respectively. Accuracy of AV was performed by using a standard sample at three different levels 80%, 100%, and 120% (54, 60, 66 μg mL^{-1}) respectively. % Recovery ± RSD was found to be 99.280 ± 0.239–101.420 ± 0.092. % Assay ± RSD was found to be (99.430–102.040) ± 0.997. Hence the developed method can be further used for estimation of AV in tablet formulation without the interference of excipients. The similar forced degradation conditions were applied for marketed formulations and found

alike method sensitivity and specificity towards APIs, degradation products, and impurities.

3.7. Marketed formulation degradation

The developed LC-MS/MS method was applied for marketed tablet formulation *(AVANA*). Avana tablet was subjected to acid, alkaline, photolytic, thermal, and oxidative degradation. Overlay chromatogram of AV and its marketed formulation in different stress condition (**Supplementary scheme S7**) shows a similar pattern to that of API. The peaks were also confirmed through LC-MS/MS and RRT. Hence developed method is useful for the determination of drug from the formulation and can extend up to toxicity study.

4. Conclusion

The stated study was able to explore various useful information which is reported for the first time in the literature for AV as separation of sixteen new D.P.s along with AV in sole LC-MS/MS compatible method, MS^n study of AV, mass fragmentation pathway of all D.P.s using LC-MS/MS and plausible degradation pathway in different conditions. Total D.P.s found in different conditions like acid, alkaline, neutral, oxidative, photolytic, and thermal were studied by LC-MS/MS. Found D.P.s were in the acid condition D.P. I, III, IV, VIII, XI, XIII and XIV; in alkaline condition D.P. I, III, IV, VIII, XI, XIII, XIV and XV; in neutral condition D.P.s I, III, IV, VIII, XIII and XIV; in oxidative degradation D.P.s VI, XII, XIII, and XIV; in photolytic degradation D.P. II, V, VII, X, XIII, XIV and XVI and in thermal degradation D.P. II, V, IX, XIII, and XIV. All sixteen degradation product structures were proposed from the data of product ion and fragment ions of LC-MS/MS. Further plausible degradation mechanism of AV in acid, alkaline, oxidative, photolytic and thermal degradation conditions were proposed which reveals that AV degradation occurs due to nucleophilic substitution reaction and amide hydrolysis. The amide group in structure can easily undergo hydrolysis, while due to aryl chloro and hydroxide group it undergoes photodecomposition. In silico toxicity prediction reveals that physicochemical properties of impurities were within the acceptable limit which specifies that no impurity is at any risk of toxicity. In detail stability study of AV revels that the drug is more prone to degrades in light, temperature, and moisture, hence it requires proper storage condition; temperature below 25 °C with protection to light and moisture.

Acknowledgement

The authors would like to thank the Institute of Pharmacy, Nirma University, India for providing necessary facilities for this work.

Funding Source

The Institute of Pharmacy, Nirma University, India provided junior research fellowship (JRF) and senior research fellowship (SRF) (NU/IP/Ph.D./FT/Stipend/14-15/003) for this work.

Appendix A. Supplementary material

Supplementary data to this article can be found online at https://doi.org/10.1016/j.arabjc.2020.06.007.

References

Bakshi, M., Singh, S., 2002. Development of validated stability-indicating assay methods: critical review. J. Pharm. Biomed. Anal. 28, 1011–1040. https://doi.org/10.1016/S0731-7085(02)00047-X.

Bandichhor, R., 2014. Identification and Characterization of Potential Impurities of Dronedarone Hydrochloride.

Bhumik, B., Kashyap, R., Buddhadev, S., 2015. Stability indicating analytical method development and validation for the estimation of Avanafil in pharmaceutical dosage form. Int. J. Pharm. Qual. Assur. 3, 181–194.

Can, N.Ö., 2018. Development of validated and stability indicating LC-DAD and LC-MS / MS Methods for Determination of Avanafil in Pharmaceutical Preparations and Identification of novel degradation product by LCMS-IT-TOF. Molecules 23, 1–14. https://doi.org/10.3390/molecules23071771.

Ferguson, J.E., Carson, C.C., 2013. Phosphodiesterase type 5 inhibitors as a treatment for erectile dysfunction: current information and new horizons. Arab J. Urol. 11, 222–229. https://doi.org/10.1016/j.aju.2013.07.009.

ICH, H. tripartite guideline, 2005a. Stability Testing of new drug substances and products Q1A (R2). http://www.ich.org/products/guidelines/quality/article/quality-guidelines.html (accessed December 18, 2016).

ICH, H. tripartite guideline, 2005b. Validation of Analytical methods definations and terminology Q2A. http://www.ich.org/products/guidelines/quality/article/quality-guidelines.html (accessed December 18, 2016).

Jain, D., Basniwal, P.K., 2013. Forced degradation and impurity profiling: recent trends in analytical perspectives. J. Pharm. Biomed. Anal. 86, 11–35. https://doi.org/10.1016/j.jpba.2013.07.013.

Jung, J., Choi, S., Cho, S.H., Ghim, J.L., Hwang, A., Kim, U., Kim, B.S., Koguchi, A., Miyoshi, S., Okabe, H., Bae, K.S., Lim, H.S., 2010. Tolerability and pharmacokinetics of avanafil, a phosphodiesterase type 5 inhibitor: a single- and multiple-dose, double-blind, randomized, placebo-controlled, dose-escalation study in healthy Korean male volunteers. Clin. Ther. 32, 1178–1187. https://doi.org/10.1016/j.clinthera.2010.06.011.

Kalariya, P.D., Patel, P.N., Sharma, M., Garg, P., Srinivas, R., Talluri, M.V.N.K., 2015a. Characterization of stress degradation products of blonanserin by UPLC-QTOF-tandem mass spectrometry. RSC Adv. 5, 69273–69288. https://doi.org/10.1039/c5ra10641a.

Kalariya, P.D., Sharma, M., Garg, P., Thota, J.R., Ragampeta, S., Talluri, M.V.N.K., 2015b. Characterization of stress degradation products of mirabegron using UPLC-QTOF-MS/MS and in silico toxicity predictions of its degradation products. RSC Adv. 5, 31024–31038. https://doi.org/10.1039/C5RA01711D.

Kotera, J., Mochida, H., Inoue, H., Noto, T., Fujishige, K., Sasaki, T., Kobayashi, T., Kojima, K., Yee, S., Yamada, Y., Kikkawa, K., Omori, K., 2012. Avanafil, a potent and highly selective phosphodiesterase-5 inhibitor for erectile dysfunction. J. Urol. 188, 668–674. https://doi.org/10.1016/j.juro.2012.03.115.

Kumar, N., Sangeetha, D., Kalyanraman, L., Sainath, K., 2017. Stability-indicating HPLC method for simultaneous determination of degradation products and process-related impurities of avanafil in avanafil tablets. Acta Chromatogr. 1–6. https://doi.org/10.1556/1326.2017.00116.

Kurmi, M., Kushwah, B.S., Sahu, A., Narayanam, M., Singh, S., 2016. Stability behaviour of antiretroviral drugs and their combinations.

2: characterization of interaction products of lamivudine and tenofovir disoproxil fumarate by mass and NMR spectrometry. J. Pharm. Biomed. Anal. 125, 245–259. https://doi.org/10.1016/j.jpba.2016.03.039.

Li, J., Zhang, D., Hu, C., 2014. Characterization of impurities in cefpodoxime proxetil using LC–MSn. Acta Pharm. Sin. B 4, 322–332. https://doi.org/10.1016/j.apsb.2014.06.007.

Mangukiya, M., Rathod, B., Dhaduk, D., Maniya, J., 2014. Development and validation of a reversed phase HPLC method for simultaneous determination of Avanafil and Dapoxetine hydrochloride in combined pharmaceutical formulation. Pharma Anal. Qual. Assur.

Modhave, D.T., Handa, T., Shah, R.P., Singh, S., 2011. Stress degradation studies on lornoxicam using LC, LC-MS/TOF and LC-MSn. J. Pharm. Biomed. Anal. 56, 538–545. https://doi.org/10.1016/j.jpba.2011.06.012.

Narayanam, M., Handa, T., Sharma, P., Jhajra, S., Muthe, P.K., Dappili, P.K., Shah, R.P., Singh, S., 2013. Critical practical aspects in the application of liquid chromatography-mass spectrometric studies for the characterization of impurities and degradation products. J. Pharm. Biomed. Anal. 87, 191–217. https://doi.org/10.1016/j.jpba.2013.04.027.

Narayanam, M., Singh, S., 2014. Characterization of stress degradation products of fosinopril by using LC-MS/TOF, MSn and on-line H/D exchange. J. Pharm. Biomed. Anal. 92, 135–143. https://doi.org/10.1016/j.jpba.2014.01.010.

Patel, M.N., Kothari, C.S., 2016. Multivariate approaches for simultaneous determination of avanafil and dapoxetine by UV chemometrics and HPLC-QbD in binary mixtures and pharmaceutical product. J. AOAC Int. 99, 649–663.

Ramesh, T., Nageswara Rao, P., Nageswara Rao, R., 2014. LC-MS/MS characterization of forced degradation products of zofenopril. J. Pharm. Biomed. Anal. 88, 609–616. https://doi.org/10.1016/j.jpba.2013.10.018.

Rao, R.N., Ramachandra, B., Sravan, B., Khalid, S., 2014. LC-MS/MS structural characterization of stress degradation products including the development of a stability indicating assay of Darunavir: An anti-HIV drug. J. Pharm. Biomed. Anal. 89, 28–33. https://doi.org/10.1016/j.jpba.2013.10.007.

Savaliya, S.D., Chaudhary, A.B., Rathod, B.G., Dobariya, T.D., Mohan, S., 2013. Development and Validation of UV Spectrophotometric method for estimation of Avanafil in tablet dosage form. Inven. Rapid Pharm Anal. Qual. Assur.

Shankar, G., Borkar, R.M., Udutha, S., Kanakaraju, M., Sai Charan, G., Misra, S., Srinivas, R., 2019. Identification and structural characterization of the stress degradation products of omeprazole using Q-TOF-LC-ESI-MS/MS and NMR experiments: Evaluation of the toxicity of the degradation products. New J. Chem. 43, 7294–7306. https://doi.org/10.1039/c9nj00932a.

Singh, S., Handa, T., Narayanam, M., Sahu, A., Junwal, M., Shah, R. P., 2012. A critical review on the use of modern sophisticated hyphenated tools in the characterization of impurities and degradation products. J. Pharm. Biomed. Anal. 69, 148–173. https://doi.org/10.1016/j.jpba.2012.03.044.

Srinivasu, P., SubbaRao, D.V., Vegesna, R.V.K., Sudhakar Babu, K., 2010. A validated stability-indicating LC method for acetazolamide in the presence of degradation products and its process-related impurities. J. Pharm. Biomed. Anal. 52, 142–148. https://doi.org/10.1016/j.jpba.2009.12.011.

Zurawin, J.L., Stewart, C.A., Anaissie, J.E., Yafi, F.A., Hellstrom, W. J.G., 2016. Avanafil for the treatment of erectile dysfunction. Expert Rev. Clin. Pharmacol. 9, 1163–1170. https://doi.org/10.1080/17512433.2016.1212655.